Mon. Not. R. Astron. Soc. **320**, 131–138 (2001)

Discs and the 10-μm silicate spectra of young stellar objects with non-photospheric continua

J. E. Bowey★† and A. J. Adamson★‡
Centre for Astrophysics, University of Central Lancashire, Preston PR1 2HE

Accepted 2000 August 6. Received 2000 June 5; in original form 2000 January 20

ABSTRACT

Dust emission in the non-photospheric 10-μm continua of HL Tau and Taurus-Elias 7 (Haro6-10, GV Tau) is distinguished from foreground silicate absorption using a simple disc model with radial power-law temperature and mass–density distributions based on the IR–submm model of T Tauri stars by Adams, Lada & Shu with foreground extinction. The resulting 10-μm absorption profiles are remarkably similar to those of the field star Taurus-Elias 16 obtained by Bowey, Adamson & Whittet. The fitted temperature indices are 0.44 (HL Tau) and 0.33 (Elias 7) in agreement with Boss's theoretical models of the 200–300 K region, but lower than those of IR–submm discs (0.5–0.61; Mannings & Emerson); a significant fraction of the modelled 10-μm emission of HL Tau is optically thin, whilst that of Elias 7 is optically thick. We suggest that HL Tau's optically thin component arises from silicate dust within low-density layers above an optically thick disc.

Key words: circumstellar matter – stars: formation – stars: pre-main-sequence – dust, extinction – infrared: stars.

1 INTRODUCTION

The 10-μm spectra of low-mass young stellar objects (YSOs) provide an opportunity to study the physical properties of the 150–500 K regions of systems analogous to the Solar nebula and the mineralogy of silicate dust in their cooler outer regions and foreground molecular cloud. The spectrum observed depends on the mass of the protostar, the density of material in its local environment, and the orientation of the YSO with respect to the observer, as well as the chemistry and density of the foreground molecular cloud. Hence the silicate spectra of YSOs vary widely (see, e.g., Hanner, Brooke & Tokunaga 1995, hereafter HBT95, 1998) and are characterized by non-photospheric emission from dust at a range of temperatures resulting in optically thin silicate emission (e.g., Taurus-Elias 1; Hanner, Brooke & Tokunaga 1994), net silicate absorption features (e.g., Taurus-Elias 7, HL Tau) or no silicate feature; sometimes these continua also contain a photospheric component (e.g., Taurus-Elias 18; Bowey, Adamson & Whittet 1998, hereafter Paper I).

Since the wavelength variation of silicate absorption is similar to that of silicate emission (and theoretically identical if the grains responsible for optically thin emission and foreground absorption have the same mineralogy and grain-size distribution), the combination of intrinsic silicate emission at a range of temperatures subsequently hidden by silicates in the foreground molecular cloud makes the 10-μm spectra of embedded objects particularly difficult to interpret, because an estimate of the continuum of these objects is required to derive the silicate absorption profile (or vice versa). Thus any attempt to understand these spectra, apart from fitting the continuum of embedded objects by eye (e.g., the estimate of the continuum of Elias 7 by Whittet et al. 1988) requires an accurate model for the intrinsic emission.

Previous models have attempted to reproduce the observed spectrum rather than provide physically realistic representations of these objects. HBT95 and Hanner et al. (1998) approximated photospheric emission and dust emission in their 10-μm flux spectra by separate power laws. A power law is an appropriate representation of the Rayleigh–Jeans photospheric flux at 10 μm. However, we find that optically thin 10-μm emission from silicates is dominated by grains with a relatively small range of temperatures, ∼100–300 K, whose blackbody emission peaks nearer (or within) the 10-μm band so that the spectrum in the region of the silicate feature cannot be approximated by a single power law. The effect of silicate absorption was included in the three-component model used in Paper I to fit the spectrum of Taurus-Elias 18. However, this model failed to provide realistic fits to the rising spectrum of Elias 7 since it required a large optically thin component, implying, contrary to infrared observations (listed in Gezari et al. 1993), that its flux will fall dramatically outside the 10- and 20-μm silicate features.

★ E-mail: jeb@star.ucl.ac.uk (JEB); adamson@jach.hawaii.edu (AJA)
† Now at Department of Physics and Astronomy, University College London, Gower Street, London WC1E 6BT.
‡ Now at the UK Infrared Telescope (UKIRT), Joint Astronomy Centre, 660 N.A'ohoku Place, Hilo, HI 96720, USA.

2 THE SOURCES

2.1 Elias 7 (Haro6-10)

In the visual band Elias 7 is a non-stellar Hα emission source with Herbig–Haro emission lines (Elias 1978). Elias found that Elias 7 had variable infrared emission and a fairly low line-of-sight extinction ($A_V \sim 6$–10 mag). More recent work has shown Elias 7 to be a pre-main-sequence binary system with optical and infrared components. Ménard et al. (1993) found that their *K*-, *L*- and *M*-band images of Haro6-10 were better modelled if the two main components were supplemented by emission from a third, ~300–400 au region of nebulosity. Using Mie theory to model spectro-polarimetric data with silicate grains, they postulate the presence of an inclined (≥84°), 1000–15000 au circumbinary envelope with an axis ratio of at least 10:1, i.e., a geometrical disc aligned to the plane of the binary, and perpendicular to the axis of the known molecular outflow (e.g. Wu, Huang & He 1996). Mid-infrared images show two components (N + S). The northern component suffers deep silicate absorption; the southern does not (Van Cleve et al. 1994). The spectral type of the primary is later than K5 (Herbst, Koresco & Leinert 1995), and so a photospheric temperature of 4000 K, consistent with that of a K5V star, was used during fitting.

2.2 HL Tau

HL Tau is the brightest nearby T Tauri star in the submm and mm continuum, and has been well studied at a variety of wavelengths. Its IR–submm spectral energy distribution (SED) (Adams, Lada & Shu 1988; Adams, Emerson & Fuller 1990) indicates the presence of a circumstellar disc, with excess far-infrared emission due to an infalling dusty envelope. Calvet et al. (1994) invoked a rotating infalling cloud to model the SED. However, they found that additional emission from a circumstellar disc was required to produce net silicate *absorption* at 10 μm due to the infalling cloud. Both the disc and infall models neglect the effect of infrared absorption by the foreground molecular cloud.

Recent observational studies and the morphology of the HL Tau system have been reviewed by Close et al. (1997). The photosphere of the YSO is obscured by dust associated with expanding cavities perpendicular to a stable 150-au disc inclined at 67° which is accreting from an infalling envelope of radius 1200 au observed in ^{13}CO along PA ~ 135° (Hayashi, Ohashi & Miyama 1993). Flux arriving directly from the protostar is heavily reddened, since it has passed through the dense, dusty accretion disc. The disc has been observed directly using submm interferometry at 0.8 mm (Lay et al. 1994) and 2.7 mm (Mundy et al. 1996; Looney, Mundy & Welch 2000), and at radio wavelengths with the VLA (Rodriguez et al. 1994). Liu et al. (1996) imaged HL Tau in the 10-μm band, but (presumably as a consequence of silicate absorption) did not find spatially extended emission or observe a disc. Visual and near-infrared imaging reveals circumstellar nebulosity due to light scattered by cavity dust particles (*V*, *I*, *R* Stapelfeldt et al. 1995; *J*, *H*, *K′*, e.g. Beckwith & Birk 1995, Close et al.; Close et al. who also observed the shadow of its accretion disc). Presumably, cavity grains are also responsible for the 50 per cent *K′*-band polarization observed at high latitude above the disc plane by Yamashita, Hodapp & Moore (1994). The system is also the source of a collimated optical jet at PA 51°.

3 OBSERVATIONS AND REDUCTION

8–13 μm spectroscopy was carried out using CGS3 at the UK Infrared Telescope on Mauna Kea, Hawaii on 1993 November 7 (UT). Weather conditions were excellent. The spectrometer was used in low-resolution mode, producing spectra centred at 10.5 μm (see Paper I). The chop throws (for real-time sky subtraction) were 20 arcsec in a direction tailored to the object. Standard stars for flux calibration were α Tau and Sirius (HL Tau only); since α Tau has a photospheric SiO absorption band, observations ratioed to this object were flux-calibrated with the spectrum of another standard. Details of the observations and calibration are given in Paper I. Errors due to variations in telluric transparency during the period of an observation were calculated by the methods used in Paper I. Since the level (but not the shape) of the spectrum of HL Tau varied during the period of observation, this spectrum was weighted by the errors obtained after pairs of observations were normalized to the same mean level.

Since the southern component of Elias 7 is not significantly extincted by silicates, this component was subtracted from the observed spectrum before fitting the silicate feature. Its flux spectrum was estimated by extrapolating the flux ratios of the N and S components obtained by Van Cleve et al. (1994) to 13.3 μm, and interpolating them to our wavelength scale (Fig. 1); here we assume that these ratios are time-invariant. Data around 12.3 μm were excluded because the detection of 3.74-μm Pfund series emission by Sato et al. (1990) suggests that there may be non-negligible H emission in our spectrum at this wavelength.

4 THE MODEL

The model presented is based on the Adams, Lada & Shu (1988, hereafter ALS) and Mannings & Emerson (1994, hereafter ME) disc model for the IR and submm SEDs of T Tauri stars.

4.1 The disc

After ALS and ME, the dusty disc is assumed to have radial temperature and density distributions given by

$$T(r) = T_* \left(\frac{R_*}{r}\right)^q, \tag{1}$$

and

$$\Sigma(r) = \Sigma_* \left(\frac{R_*}{r}\right)^p, \tag{2}$$

respectively. T_* and Σ_* are, respectively, the temperature and

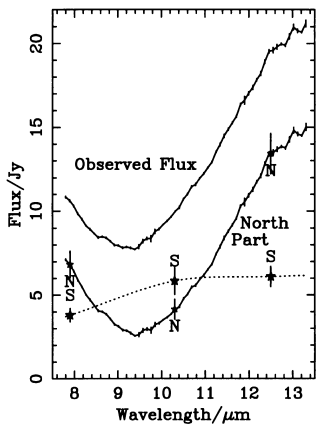

Figure 1. Subtraction of southern flux component from Elias 7.

mass densities at the stellar radius R_*; q is the index of the temperature distribution, and the mass density index, $p = 7/4$, is adopted from protostellar theory (e.g. ALS).

After ALS and ME the luminosity density, L_ν, of such a disc is

$$L_\nu = 4\pi \cos\theta \int_{R_*}^{R_D} B_\nu[T(r)][1 - e^{-\tau_\nu(r,\theta)}] 2\pi r \, dr, \quad (3)$$

where θ is the angle of inclination of the disc to the sky plane. In the optically thin case there will be a silicate emission feature, of slant optical depth $\tau_\nu(r, \theta)$, superimposed on the blackbody continuum. If the disc is optically thick, the exponential term will fall to zero and the continuum will be smooth, $\propto \int_{R_*}^{R_D} B_\nu[T(r)]\, dr$.

Our spectra extend over only 5 μm, making them sensitive to a small range in temperature. Therefore, to avoid assuming a value for R_D, we integrate over temperature instead of radius. Hence,

$$L_{\nu\,\mathrm{disc}} = \frac{8\pi^2 \cos\theta}{qT_0R_0^q} \int_{T_D}^{T_0} B_\nu(T)[1 - e^{-\tau_\nu(T,\theta)}] r(T)^{q+2}\, dT, \quad (4)$$

where $r(T)$ is obtained from equation (1), and T_0 and T_D are, respectively, the temperatures of the inner and outer edges of the region of the disc which emits in the 10-μm band.

4.1.1 *Optical depth of the silicate emission*

The emission optical depth is given by

$$\tau_\nu(r, \theta) = \frac{\kappa_\nu \Sigma(r)}{\cos\theta}, \quad (5)$$

where κ_ν, the absorption coefficient of *all* material in the disc, is given in units of $\mathrm{cm^2\,g^{-1}}$. We assume that optically thin emission in the 10-μm band is dominated by silicates so that

$$\kappa_\nu = \text{constant} \times \epsilon_\nu = k\epsilon_\nu, \quad (6)$$

where ϵ_ν is the normalized 10-μm silicate emissivity (i.e., the shape of the 10-μm silicate absorption/emission feature normalized to unity at the wavelength of its peak). After substituting for $\Sigma(r)$ from equation (2) into equation (5), the slant optical depth of the disc emission becomes

$$\tau_\nu(r, \theta) = k\epsilon_\nu \frac{\Sigma_0}{\cos\theta} \left(\frac{R_0}{r}\right)^p = c\epsilon_\nu r(T)^{-p}, \quad (7)$$

where

$$c = \frac{k\Sigma_0 R_0^p}{\cos\theta}, \quad (8)$$

and Σ_0 and R_0 are defined as the mass density and radius at the inner edge of the *silicate* disc where $T(r) = T_0$. R_0 is estimated from equation (1), with $R_* = 2\,R_\odot$, the radius of a typical T Tauri star (after ME).

4.1.2 *The disc flux*

Inserting equation (7), the expression for the slant optical depth, into equation (4), and noting that the disc flux $F_{\nu\,\mathrm{disc}} = L_{\nu\,\mathrm{disc}}/4\pi D^2$, where D is the distance to the YSO, the equation for disc flux becomes

$$F_{\nu\,\mathrm{disc}} = a \int_{T_D}^{T_0} B_\nu(T)[1 - e^{-c\epsilon_\nu r(T)^{-p}}] r(T)^{q+2}\, dT, \quad (9)$$

where a the scale of $F_{\nu\,\mathrm{disc}}$ is given by

$$a = \frac{2\pi \cos\theta}{D^2 qT_0R_0^q}. \quad (10)$$

4.2 Fitting the observed flux

The intrinsic flux of the disc is reduced by material in the cooler outer regions of the disc and foreground molecular cloud including silicates. Hence the flux *observed*, F_ν, is given by

$$F_\nu = F_{\nu\,\mathrm{disc}} e^{-\tau_{\mathrm{cont}}(\lambda)} e^{-c_{\mathrm{sil}}\epsilon_\nu}, \quad (11)$$

where c_{sil} is the optical depth of the foreground silicate absorption feature modelled with the silicate emissivity, ϵ_ν (it is assumed that the protostellar disc and molecular-cloud silicate emissivities are the same). $\tau_{\mathrm{cont}}(\lambda)$ is the continuum extinction optical depth, which is assumed (as in Paper I) to vary as a power law longwards of the H band.

$$\tau_{\mathrm{cont}}(\lambda) = \tau_{\mathrm{cont}}(1.65\,\mu\mathrm{m}) \left(\frac{\lambda}{1.65}\right)^{-1.8}, \quad (12)$$

where the exponent (-1.8) is the mean value obtained by Martin & Whittet (1990). H-band extinctions were derived from estimates of A_V, using the extinction law for the ρ Oph Molecular Cloud (Whittet 1992), since none is determined for the TMC.

To summarize, the 10-μm disc model (equation 11) differs from the IR–submm model of ALS and ME in three main ways: (i) flux is integrated over blackbody temperature instead of radius (so that the radius is not estimated from other observations); (ii) optically thin emission is modelled with a (scaled) silicate emissivity, ϵ_ν; (iii) as for the field objects (Paper I), the intrinsic emission is multiplied by terms representing foreground continuum and silicate extinction. Additionally, the scales of mass density, Σ_0, and the central radius of the disc, R_0, are estimated at the inner radius of the annulus for which $T_{\mathrm{ann}} = 1000\,\mathrm{K}$, as opposed to the stellar radius. Parameters a, q, c and c_{sil} are fitted by χ^2_ν minimization.

5 COMPUTATION

The integration over temperature was performed numerically using the Extended Trapezoidal Rule, to sum the flux emitted by 40 annuli with the temperature of the centre of the outer annulus set to 70 K (fits with 100 annuli produced identical results). χ^2 minimizations were performed using the downhill simplex method (Press et al. 1992). In preliminary fits, flux contributions from components hotter than 1000 K each contributed ≤0.1 per cent at 10 μm, whilst the fluxes due to annuli for which $T < 70\,\mathrm{K}$ were too small to calculate; hence the temperatures of the inner and outer annuli, T_0 and T_D, were set to 1000 and 70 K, respectively. Initially, optically thick [$\tau_{10.0\,\mu\mathrm{m}}(T_0, \theta) \geq 1000$] discs remained so during fitting, but better fits were obtained if the discs were initially very optically thin [$\tau_{10.0\,\mu\mathrm{m}}(T_0, \theta) < 1$].

The modelled flux and χ^2_ν are *insensitive* to changes in T_* and A_V; values of T_* and $\tau_{\mathrm{cont}}(1.65\,\mu\mathrm{m})$ in the ranges $4000 \leq T_* \leq 25\,000\,\mathrm{K}$ and $0.95 \leq \tau_{\mathrm{cont}}(1.65\,\mu\mathrm{m}) \leq 1.6$ (i.e., $6 \leq A_V \leq 10$, the range suggested for Elias 7 by Elias (1978) had no effect on the goodness of fit, the temperature index q, or the absorption optical depth c_{sil}. However, c changed with T_* to provide a constant optically thin emission component; when $T_* < 4000\,\mathrm{K}$, the fits were poorer due to the lack of an optically thin component. Due to the temperature dependence of the modelled radius, changes in T_* and $\tau_{\mathrm{cont}}(1.65\,\mu\mathrm{m})$ ($\propto A_V$) affect the apparent size of the disc; a, the scale of the flux, is larger for a smaller disc to compensate for the decrease in surface area.

Table 1. 10-μm disc model fits with astronomical and laboratory emissivities.

Source	A_V	Modelling Emissivity[a]											
		Trapezium			μ Cephei			Diopside			Simpson 1		
		q^b	c_{sil}	χ^2_ν	q^b	c_{sil}	χ^2_ν	q^b	c_{sil}	χ^2_ν	q^b	c_{sil}	χ^2_ν
Elias 7	6–10 mag	0.33	1.7	24	0.34	1.1	23	0.36	1.0	55	0.29	1.7	110
HL Tau	23 mag	0.44	1.1	9.1	0.53	0.56	15	0.57	0.47	17	0.47	0.83	31

[a] References: *Trapezium* – Forrest et al. (1975); *μ Cephei* – Russell et al. (1975); *diopside* – Blanco et al. (1993); *Simpson 1* – Simpson's group 1 circumstellar emissivity (Simpson 1991).
[b] For Elias 7 the fitted temperature index, q, is the mean for A_Vs of 6 and 10 mag. $q(A_V = 6) \sim q_{mean} - 0.01$.

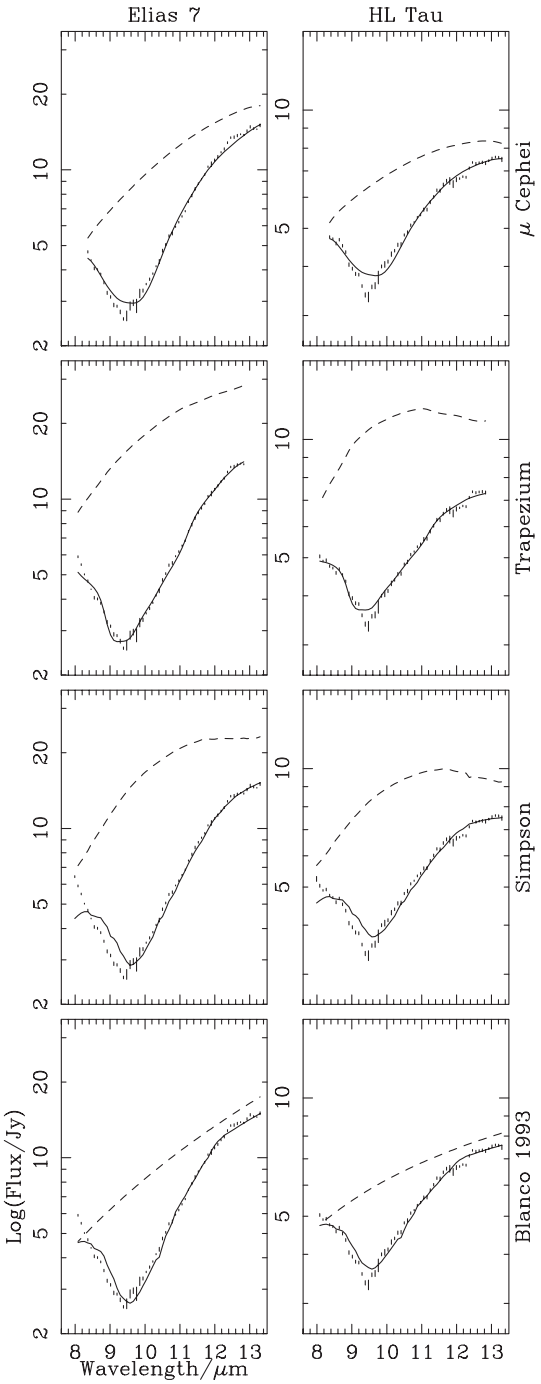

Figure 2. 10-μm flux spectra of Elias 7 and HL Tau with modelled fluxes *(solid)* and derived continua *(dashed)*. Fits were obtained with the μ Cephei, Trapezium, and Simpson emissivities and the absorption spectrum of amorphous diopside obtained by Blanco et al. (1993) (see Section 6).

5.1 Adopted extinction

HL Tau has a complicated geometry (discussed in Section 2.2). The stellar photosphere is not seen directly in the optical but, on the basis of adaptive-optics observations, Close et al. (1997) claimed to see through to the star in all three near-infrared (NIR) bands, and determined colour indices of 3.1, 2.1 and 5.3 mag in $J - H$, $H - K'$ and $J - K'$, respectively, from a point source on the scale of their adaptive-optics resolution, 0.2 arcsec. More extensive patches (including flux from the scattering cones) were significantly bluer. Since the mid-infrared disc is at most some tens of au across and at a distance of around 140 pc, the 10-μm emission region is no more than 0.2 arcsec across. It is therefore appropriate to employ the Close et al. 'point-source' measurements to estimate the foreground extinction affecting the 10-μm spectrum. Adopting a spectral type of K7V, combining the point-source colours with intrinsic colours from Tokunaga (2000), and using a dark-cloud extinction law ($R_V = 4.5$) from Whittet (1992), we infer visual extinctions of 18.5, 20.3, and 22.9 mag, respectively, from the observed $J - H$, $J - K$ and $H - K$. The trend to redder colour with mean wavelength may reflect emission from heated local dust in the K band, and/or a contribution from small-grain scattering in the J band. Tests demonstrate that the disc properties are insensitive to variations of this order in the assumed foreground A_V. We adopt the value of 23 mag in Table 2, since $H - K$ is least affected by scattering.

The NIR morphology of Elias 7 is less well known, and we simply adopted Elias's (1978) values of the visual extinction ($A_V \sim$ 6–10 mag) during fitting.

6 THE SILICATE SPECTRA

The silicate emissivities used for modelling the observed spectra (Fig. 4) are those which were found to be most similar to the absorption spectra of the TMC sources Elias 16 and 18 (Paper I). The astronomical emissivities were of dust in the Trapezium region of the Orion nebula (Forrest, Gillett & Stein 1975), the circumstellar O-rich dust around μ Cephei (Russell, Soifer & Forrest 1975) and Simpson's Group 1 *IRAS* sources (Simpson 1991); the best laboratory spectrum was of amorphous diopside with a grain size of 0.1 μm (Blanco et al. 1993). Fitted χ^2_ν are necessarily large, since the peak wavelength (λ_c) and FWHM of the modelling emissivities differ from those of TMC silicates.

6.1 The fits and continua

Fits to the flux spectra of Elias 7 North and HL Tau, together with the derived continua are shown in Fig. 2; the statistics, and fitted parameters are listed in Table 1. The flux spectra of Elias 7 North and HL Tau, like those of the Taurus Molecular Cloud (TMC)

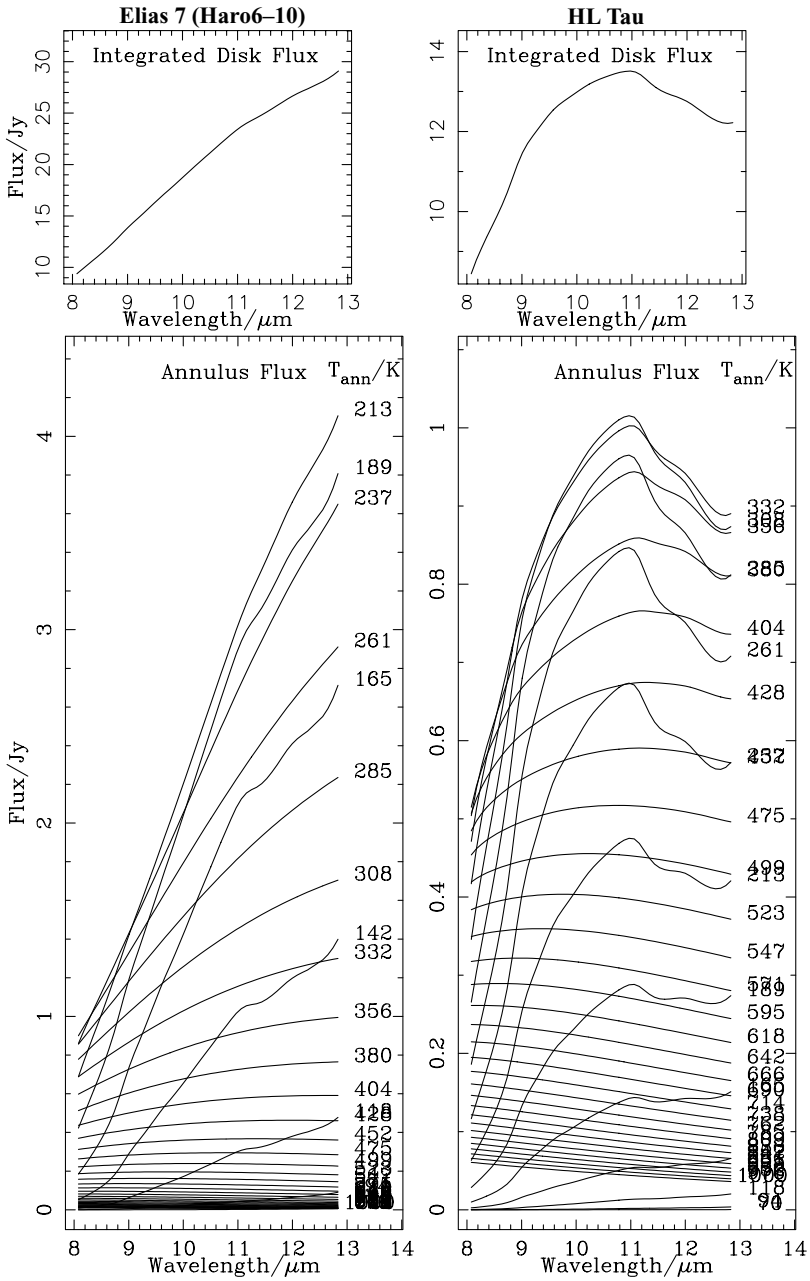

Figure 3. Top: Fitted $F_{\nu\,\mathrm{disc}}$ (equation 9) of Elias 7 and HL Tau using the Trapezium emissivity. Bottom: Annular flux components summed to produce $F_{\nu\,\mathrm{disc}}$.

sources Elias 16 and 18 (Paper I), are better fitted with the Trapezium emissivity than by μ Cephei or Simpson's Group 1 emissivity. (We judge the fit of Elias 7 with the Trapezium emissivity to be better than that with μ Cephei,[1] since the wavelength of peak absorption of the Trapezium-modelled flux is better centred on the observed feature.)

6.2 Optically thin silicate emission

Emission in the continuum of Elias 7 is optically thick irrespective of the silicate emissivity used for fitting. However, for HL Tau, all good continuum fits (i.e., excluding the poor fit obtained with diopside) indicate that the disc in this object is optically thin in regions which emit significantly in the 10-μm band. The optical depth of the silicate emission is invariant over a wide range of visual extinctions. Fits with the Trapezium emissivity and $A_V =$ 12 mag (see Bowey & Adamson 2000a), 23 and 30 mag ($q = 0.45$, $c_{\mathrm{sil}} = 1.1$, $\chi^2_\nu = 9.2$) produced nearly identical continua with the 23 and 30-mag continua varying by $\lesssim$0.4 per cent at all wavelengths. Boss & Yorke (1996) also find optically thin emission may be produced by a circumstellar disc. However, our result contrasts with ALS's assumptions of optical thickness; the inferred difference in optical thickness may be at least partially due to the use of larger beams for the infrared observations on which IR–submm models are based (our aperture was 5.5 arcsec; *IRAS* typically used ~1 arcmin). Our simple model also disagrees with the results of the radiative-transfer flared-disc calculations by

[1] The fit with μ Cephei is better at shorter wavelengths where the telluric transparency variation during the observation of Elias 7 was smallest.

Table 2. Physical results of the 10-μm disc model.

Object	Pre-set T_* K	Pre-set A_V mag	Pre-set θ °	Silicate Absorption τ_{sil}[b]	Silicate Absorption N_{sil}[c] mol cm^{-2}	F_{pk} Jy	ΔT K	Disc Parameters[a] $\Delta\tau_{emiss}$	R_0 au	R_{pk} au	R_{sil} au	Σ_0 g cm^{-2}
Elias 7	4000	6	85	1.7	5.4×10^{18}	2.2	150–360	0.97–100	0.73	110	410	0.81
		10				2.2	150–370	1.0–110	0.68	99	350	0.68
HL Tau	4000	23	67	1.1	3.2×10^{18}	0.95	200–550	0.51–24	0.23	3.9	11	0.036

[a] ΔT and $\Delta\tau_{emiss}$ are, respectively, the ranges of annular temperature and 10.0 μm emission optical depths for which $F_{ann} \geq e^{-1} \times F_{pk}$; R_0 is the inner radius of the 1000-K annulus; R_{pk} is the outer radius of the annulus which produces the largest flux component at 10.0 μm; R_{sil} is the outer radius of the *silicate* disc where $F_{ann} = e^{-1} \times F_{pk}$.
[b] Optical depth at the wavelength of the peak of the unnormalized silicate absorption feature.
[c] Silicate column density ≃ full-width-half-maximum of silicate absorption feature $\times \tau_{sil}/\sigma_{int}$, for which the integrated band cross-section, $\sigma_{int} = 1.1 \times 10^{-18}$ cm^2 μm molecule^{-1} for $\lambda_c = 9.7$ μm (Skinner et al. 1992).

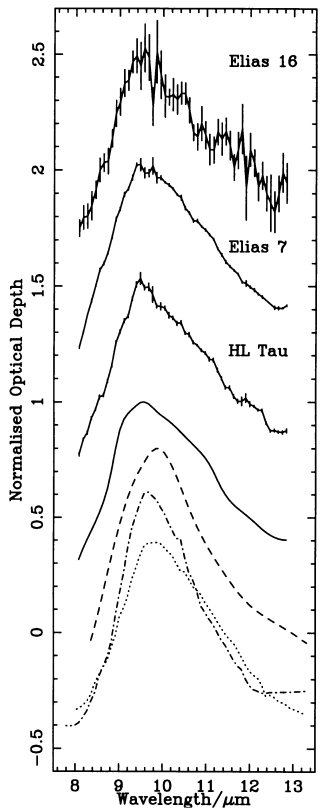

Figure 4. Normalized 10-μm optical depth profiles of TMC dust: Elias 16 (Paper I) – quiescent molecular cloud; Elias 7 and HL Tau – YSO and foreground molecular cloud. Modelling emissivities: Trapezium *(solid)*, μ Cephei *(dashed)*, diopside *(dot-dash-dot)*, Simpson's group 1 *(dotted)*. Offsets are −0.6,−0.4,−0.2, 0.0, 0.5, 1.0 and 1.5, respectively.

Men'shchikov, Henning & Fischer (1999), Men'shchikov et al. find that 100-μm-sized grains in a central torus which is optically thick beyond mm wavelengths best match HL Tau's beam-matched optical-mm SED. Their model reproduces the shape of the 10-μm absorption feature, but the 5–20 μm fluxes are ∼50 per cent too large. We suggest that the optically thin component of our fits may be due to low-density layers of grains on the surface of an optically thick disc.

The undimmed continua and contributions of individual annuli to the modelled intrinsic emission of Elias 7 and HL Tau are shown in Fig. 3. The optically thin emission components of HL Tau peak at ∼11 μm, whilst the featureless optically thick components of Elias 7 rise with increasing wavelength. Ripples in some of the Elias 7 annular components (for which $T_{ann} \lesssim 190$ K) are due to insignificant optically thin emission which is probably required to smooth out bumps in the Trapezium emissivity.

If the silicate emission bands of YSOs are indeed optically thin, the protostellar models may need modification since most assume disc emission to be optically thick in the mid-infrared. The effect of substantial differences in the opacity of the emitting disc has not been explored by theorists. Boss varied opacity by factors of 3 in the 200–700 K region, and obtained minimal effects on the temperature profile and mid-infrared fluxes.

6.3 Silicate absorption profiles

The derived absorption profiles of HL Tau, Elias 7 and the TMC field star Elias 16 (reproduced from Paper I) are compared in Fig. 4. The similarity of these silicate profiles suggests that the 10-μm disc model has successfully separated the 10-μm emission and absorption components. Bowey & Adamson (2000b,c) use these, and other, 10-μm silicate profiles to deduce the mineralogy of TMC silicate dust.

The peak optical depths of the absorption profiles obtained with the disc model are larger than those found by Whittet et al., who obtained $\tau_{9.7} = 0.87$ and 0.71 for Elias 7 and HL Tau, respectively. The silicate optical depth, τ_{sil}, towards Elias 16 is only 0.81, giving a silicate column density, N_{sil}, of 2.4×10^{18} mol cm^{-2} (Paper I) despite a relatively high A_V of 22.3 mag (Chiar et al. 1995). If the extinction towards HL Tau is ∼23 mag, this implies $\gtrsim 0.8 \times 10^{18}$ mol cm^{-2} of the cold silicates responsible for the absorption feature are associated with the YSO, in addition to the warmer grains seen in the optically thin emission feature. Thus, assuming that the density of the quiescent TMC is fairly uniform, the density of submicron-sized silicate grains in the YSO environment is significantly higher than that in the quiescent molecular cloud.

7 PHYSICAL PARAMETERS OF THE DISCS

The ranges in temperature and optical depth of significant annular flux components for which $F_{ann} \geq F_{pk}/e$, where F_{pk} is the largest annular flux component at 10.0 μm, and e is the base of natural logarithms, are given in Table 2. The 10-μm spectra of these objects are most sensitive to temperatures in the 200–400 K range. We believe our simple model to be a reasonable representation of these systems (HL Tau in particular), because the silicate profiles

are similar to those of less complicated environments and the YSO parameters obtained for the infrared are consistent with previous results.

7.1 Fitted temperature index, *q*

The fitted temperature indices, $q = 0.33$ and 0.44, for Elias 7 and HL Tau, respectively, are just below those of active ($q = 0.5$) discs, and lower than the 0.5–0.61 range obtained by ME using the IR–submm ALS disc model. However, our results are consistent with the mid-infrared temperature distribution produced by Boss's protoplanetary disc models for T Tau (Boss & Yorke 1996). In these models the radial power-law temperature distribution of ALS is modified in the disc mid-plane ($1 \leq r \leq 10$ au) by the effects of grain condensation and evaporation on opacity, causing $T(r)$ to plateau at radii of ~2–4 au, corresponding to the 200–300 K temperature range. Boss (1996) found, as did we, that altering the stellar temperature had no effect on the index and mid-temperature flattening of the radial temperature profile. The uniform radial temperature distribution has also been challenged at radio wavelengths in infall-plus-disc models of YSOs (D'Alessio, Calvet & Hartmann 1997).

7.2 Apparent size of the discs at 10 μm

Assuming that the radial temperature distribution is uniform between 8 and 13 μm, we may estimate the size of the modelled disc in the 10-μm band using equation (1). We define the radius of the disc when $\lambda = 10$ μm, $R_{\rm sil}$, to be that where the flux falls below one scaleheight of $F_{\rm pk}$. (Thus the radius of peak emission is $R_{\rm pk}$.) Therefore the region of the disc which makes a significant contribution to the flux will have blackbody temperatures in the ~200–400 K range. It is important to remember, however, that these sizes depend critically on parameters that are difficult to determine for embedded objects, namely the estimated photospheric temperature, stellar radius and visual extinction, with the largest uncertainty being in A_V.

The inferred radii of the 10-μm discs for the estimated ranges of A_V are given in Table 2. The ~400-au 10-μm disc of Elias 7 is consistent with the flattened circumbinary envelope proposed by (Ménard et al. 1993) to explain extended emission in their *K*-, *L*- and *M*-band images of the system. In the *L* band (3.6 μm) the radius of our disc would be about 20 au, or ~0.14 arcsec (from the ratio of the respective *L*- and *N*-band blackbody peaks of 800 and 300 K), which roughly coincides with the 75 per cent contour of the *L*-band residual emission obtained by Ménard et al. Our estimate for HL Tau's radius is not consistent with submm estimates. Equation (1) predicts the radius of the 34-K annulus to be ~500 au,[2] with our fitted value of $q = 0.44$. However, Adams et al. (1990) obtain 100 au at 34 K using the ALS method (with $q = 0.501$, $R_* = 1.6\,{\rm R}_\odot$); replacing R_* with our value of $2\,{\rm R}_\odot$, this becomes 125 au. 2.7-mm images indicate disc sizes of 70 ± 15 au (Mundy et al. 1996), and fits to the flux with the density index, $p \lesssim 1.0$, indicate outer radii in the 90–160 au range; submm fits with $p > 1.0$ result in larger discs and poorer fits. In contrast, disc-model fits to the 10-μm spectrum with $p = 0.5$ result in a poorer fit ($\chi^2_\nu = 11$), a steeper temperature index ($q = 0.55$), and a smaller ($R_{\rm pk} = 1.0$ au, $R_{\rm sil} = 3$ au) and hotter (180–700 K) silicate disc with less foreground absorption ($c_{\rm sil} = 0.93$).

The agreement of NIR data and disagreement of the submm result with the 10-μm estimate is consistent with the flattening of the 200–300 K profile (discussed in Section 7.1) and our hypothesis that the silicate emission arises from optically thin layers above an optically thick disc.

7.3 Estimates of the scale of mass column density, Σ_0

The modelled 10-μm disc of HL Tau is optically thin. Since the absorption coefficient, κ_ν, is measured for laboratory smokes at 9.7 μm: $\kappa_{9.7} = k\epsilon_\nu = 3000\,{\rm cm^2\,g^{-1}}$ (Dorschner & Henning 1986), and the normalized silicate emissivity function, $\epsilon_\nu = 1$, at the wavelength of its peak (typically $\lambda = 9.7 \pm 0.3$ μm), equation (8) may be reduced to

$$c = \kappa_{9.7}\,\frac{\Sigma_0 R_0^p}{\cos\theta} \tag{13}$$

near to λ_c. Hence, by substituting fitted values of c and R_0 into equation (13), and using published estimates of the disc inclination, θ, we obtain the values for the scale of the mass density due of silicates, Σ_0, which are given in Table 2. The estimated mass of silicate dust ($\approx \pi 8 R_0^p R_{\rm submm}^{2-p}\Sigma_0$, where $p = 7/4$; see ME) in the 125-au IR–submm disc of HL Tau is extremely low at $2.6 \times 10^{-8}\,{\rm M}_\odot (\equiv 0.0087\,{\rm M}_\oplus)$. Even assuming the canonical gas-to-dust ratio of ~100, this mass is $\sim 10^{-6}\,{\rm M}_\odot$ compared with the 1.0-$M_\odot$ estimate of Adams et al. (1990). This low estimate may also indicate that the optically thin component of silicate emission derives from grains in low-density layers rather than the main disc. We also note that, since the ALS model assumes uniform radial power-law temperature and mass–density indices throughout the IR–submm disc, neglects the effects of infall on the submm flux, and assumes that the 10-μm emission is optically thick, their estimate may be too large. Both these simple models also ignore disc flaring. Given the complexity of the system, estimates of disc mass cannot be obtained from fits with the 10-μm disc model.

8 SUMMARY

Dust emission in the non-photospheric 10-μm continuum of HL Tau and Taurus-Elias 7 (Haro6-10) is distinguished from foreground silicate absorption using a 10-μm disc model with radial power-law temperature and mass–density distributions based on the IR–submm model of T Tauri stars by ALS with terms for foreground extinction.

We find that the Trapezium emissivity better represents the silicate feature towards these embedded objects than those of the other emissivities used for fitting (μ Cephei, Simpson's Group 1 and diopside) matching the result for TMC field stars (Paper I).

With the assumed Trapezium emissivity, the intrinsic dust emission of HL Tau is significantly optically thin at 10 μm, whilst that of Elias 7 is optically thick. The optically thin emission in fits to HL Tau may be due to low-density layers at the surface of an optically thick disc.

The fitted continua result in deep silicate absorption features $\tau_{\rm sil} = 1.7$ (Elias 7) and 1.1 (HL Tau), whose normalized profiles are very similar to that of the field object Taurus-Elias 16.

The fitted continuum, temperature index, q, and resulting

[2] This is not well constrained, since the annular temperature increment is 23.8 K and the temperature change is slow in the submm. The inner and outer radii of the 34-K annulus would be ~300 and ~4500 au, respectively.

silicate absorption profile are insensitive to preset values of continuum optical depth and photospheric temperature, T_*. For Elias 7 and HL Tau, the fitted values of $q = 0.33$ and 0.44, respectively, are lower than those obtained for IR–submm discs by ME for which $q \sim 0.5$–0.61; this result is consistent with the flattened 200–300 K profile caused by dust evaporation and condensation in the standard model of Boss (1996).

Other disc parameters depend on pre-determined and (currently) relatively uncertain estimates of photospheric temperature and A_Vs, based on near-infrared observations. For A_Vs of 6–10 mag and $T_* = 4000$ K, the extent of Elias 7's 350–410 au 10-μm disc is consistent with the size of the flattened circumbinary envelope in the K to L bands proposed by (Ménard et al. 1993). However, the submm ($T_{\rm ann} = 34$ K) radius of the 11 au 10-μm disc of HL Tau (with $T_* = 4000$ K, $A_V = 23$ mag) would be ~500 au, inconsistent with the Adams et al. (1990) estimate of 125 au (after adopting our value of $R_* = 2\,R_\odot$).

ACKNOWLEDGMENTS

This work is based on data obtained with the UK Infrared Telescope, Mauna Kea Observatory, Hawaii, reduced and analysed using Starlink facilities. AJA was funded jointly by the University of Central Lancashire and the UK Starlink project. This work is included in JEB's PhD thesis; her studentship was funded primarily by the University of Central Lancashire, and additionally by a small grant from the British Fellowship of Women Graduates. The authors thank D. C. B. Whittet for suggesting the astronomical silicates PhD project, and the anonymous referee for a constructive report.

REFERENCES

Adams F. C., Lada C. J., Shu F. H., 1988, ApJ, 326, 865(ALS)
Adams F. C., Emerson J. P., Fuller G. A., 1990, ApJ, 357, 606
Beckwith S. V. W., Birk C. C., 1995, ApJ, 449, L59
Blanco A., Fonti S., Martino M., Bussoletti E., Mennella V., Colangeli L., Stephens J. R., 1993, ASP Conf. Ser. Vol. 41, 267
Boss A. P., 1996, ApJ, 469, 906
Boss A. P., Yorke H. W., 1996, ApJ, 469, 366
Bowey J. E., Adamson A. J., 2000a, in Sitko M. L., Sprague A. L., Lynch D. K., eds, Thermal Emission Spectroscopy and Analysis of Dust, Discs, and Regoliths, ASP Conf. Ser., Vol. 196. Astron. Soc. Pac., San Francisco, p. 83
Bowey J. E., Adamson A. J., 2000b, in Sitko M. L., Sprague A. L., Lynch D. K., eds, Thermal Emission Spectroscopy and Analysis of Dust, Discs, and Regoliths, ASP Conf. Ser., Vol. 196. Astron. Soc. Pac., San Francisco, p. 31
Bowey J. E., Adamson A. J., 2000c, ApJ, submitted,
Bowey J. E., Adamson A. J., Whittet D. C. B., 1998, MNRAS, 298, 131 (Paper I)
Calvet N., Hartmann L., Kenyon S. J., Whitney B., 1994, ApJ, 434, 330
Chiar J. E., Adamson A. J., Kerr T. H., Whittet D. C. B., 1995, ApJ, 455, 234
Close L. M., Roddier F., Northcott M. J., Roddier C., Graves J. E., 1997, ApJ, 478, 766
D'Alessio P., Calvet N., Hartmann L., 1997, ApJ, 474, 397
Dorschner J., Henning T., 1986, Ap&SS, 128, 47
Elias J. H., 1978, ApJ, 224, 857
Forrest W. J., Gillett F. C., Stein W. A., 1975, ApJ, 195, 423
Gezari D. Y., Schmitz M., Pitts P. S., Mead J. M., 1993, NASA Ref. Publ., 1294
Hanner M. S., Brooke T. Y., Tokunaga A. T., 1994, ApJ, 433, L97
Hanner M. S., Brooke T. Y., Tokunaga A. T., 1995, ApJ, 438, 250 (HBT95)
Hanner M. S., Brooke T. Y., Tokunaga A. T., 1998, ApJ, 502, 871
Hayashi M., Ohashi N., Miyama S. M., 1993, ApJ, 418, L71
Herbst T. M., Koresco C. D., Leinert C., 1995, ApJ, 444, L93
Lay O. P., Carlstrom J. E., Hills R. E., Phillips T. G., 1994, ApJ, 434, L75
Liu M. C. et al., 1996, ApJ, 461, 334
Looney L. W., Mundy L. G., Welch W. J., 2000, ApJ, 529, 477
Mannings V., Emerson J. P., 1994, MNRAS, 267, 361 (ME)
Martin P. G., Whittet D. C. B., 1990, ApJ, 357, 113
Ménard F., Monin J., Angelucci F., Rouan D., 1993, ApJ, 414, L117
Men'shchikov A. B., Henning Th., Fischer O., 1999, ApJ, 519, 527
Mundy L. G. et al., 1996, ApJ, 464, L169
Press W. H., Teukolsky S. A., Vetterling W. T., Flannery B. P., 1992, *Numerical Recipes in FORTRAN*. Cambridge Univ. Press, Cambridge
Rodriguez L. F., Canto J., Torrelles J. M., Gomez J. F., Anglada G., Ho P. T. P., 1994, ApJ, 427, L103
Russell R. W., Soifer B. T., Forrest W. J., 1975, ApJ, 198, L41
Sato S., Nagata T., Tanaka M., Yamamoto T., 1990, ApJ, 359, 192
Simpson J. P., 1991, ApJ, 368, 570
Skinner C. J., Tielens A.G.G.M., Barlow M. J., Justtanont K., 1992, ApJ, 399, L79
Stapelfeldt K. R. et al., 1995, ApJ, 449, 888
Tokunaga A. T., 2000, in Cox A. N., ed., Allen's Astrophysical Quantities, 4th edn. Springer-Verlag, New York, p. 143
Van Cleve J. E., Hayward T. L., Miles J. W., Gull G. E., Shoenwald J., Houck J. R., 1994, Ap&SS, 212, 231
Whittet D. C. B., 1992, *Dust in the Galactic Environment*. IOP Publishing Ltd.
Whittet D. C. B., Bode M. F., Longmore A. J., Adamson A. J., McFadzean A. D., Aitken D. K., Roche P. F., 1988, MNRAS, 233, 321
Wu Y., Huang M., He J., 1996, A&AS, 115, 283
Yamashita T., Hodapp K. W., Moore J. T., 1994, ApJ, 422, L21

This paper has been typeset from a TEX/LATEX file prepared by the author.